

# Determination of Charpy transition temperature of ferritic steels using miniaturized specimens

M. P. MANAHAN

*The Pennsylvania State University\*, 231 Sackett Building, University Park, PA, 16802, USA*

Miniaturized specimen technology permits mechanical behaviour to be determined using a minimum volume of material. A method for obtaining the ductile-brittle transition temperature of ferritic steels was developed using a miniaturized notched bar test. Comparisons between conventional and miniaturized specimen ductile-brittle transition temperatures are encouraging. Fracture toughness values were calculated for the miniaturized notched specimens and compared with large-specimen data. The miniaturized specimen values were high, even after appropriate adjustments had been made. Further development may yield valid data when an optimum combination of specimen size, shape, and notch acuity is determined.

## 1. Introduction

Because miniaturized specimen technology (MST) permits characterization of mechanical behaviour using a minimum volume of material, it has many applications, such as nuclear pressure vessel surveillance, failure analysis, and post-irradiation testing [1]. It can also be used to characterize the mechanical behaviour of in-service structures and components in cases where small pieces of material can be cut out safely. The goal of the present study was to examine the feasibility of a fracture mechanics test making use of miniaturized three-point-bend (TPB) specimens. A test was developed to determine the ductile-brittle transition temperature (DBTT) of ferritic steel. An attempt was also made to determine plane-strain fracture toughness ( $K_{Ic}$ ) from the miniaturized notched specimens. The determination of  $K_{Ic}$  requires an optimum combination of miniaturized specimen size, shape and notch acuity, which has not as yet been found.

### 1.1. Review of the literature

Partly as a result of the high incidence of brittle fracture failures in the steel of the Liberty merchant ships of the US Navy during World War II, a great interest arose in the development of a simple, cost-effective laboratory test capable of evaluating the susceptibility of steels to brittle fracture. An extensive body of literature has developed over the past 40 years that addresses size and geometry effects on DBTT determination. Many different test methods such as impact tests, drop-weight tests and dynamic tear tests have been developed to simulate service conditions. Current fracture behaviour tests that grew out of this large body of data are discussed in detail in the ASTM standards [2-13].

The Charpy V-notch (CVN) impact test, one of the simplest fracture behaviour tests, yields a variety of data, including impact energy, lateral expansion and percentage of ductile fracture area as a function of test

temperature. The test is usually conducted over a range of temperatures, within which the transition from brittle to ductile fracture occurs. Previous studies have attempted to isolate the factors that influence DBTT [14-40].

Recent work, most notably that of Corwin and Houghland [41], Lucas *et al.* [42] and McConnell *et al.* [43], has indicated that CVN tests, including those for miniaturized specimens, provide only empirical or qualitative data. These authors conclude that the mini-CVN tests have been found valuable for determining material considerations such as fundamental fracture and flow parameters, the validity of interpolative fracture criteria, valid fracture toughness fibrous crack growth resistance curves, and qualitative data for tracking irradiation behaviour and monitoring relative differences of materials. ASTM Standard A370-86a [2] suggests that the energy values determined by these tests are "qualitative comparisons . . . [that] cannot be converted into energy figures that would serve for engineering calculations". Further, Lucas *et al.* [42] state that:

"Thus while the behaviour of mini-CVN specimens has been found to be qualitatively similar to that of standard CVNs, quantitative comparisons have been found to be only in approximate agreement at best. This is not particularly surprising, since parameters such as transition temperature or  $\Delta TT$  are functions of an arbitrarily chosen reference energy and are thus sensitive to test conditions and particularly specimen geometry. Thus it would seem that the greater potential for success in using mini-CVNs is to use them to extract more fundamental property information" [41].

The present study advances and extends the current theory of mini-CVN testing to obtain from miniaturized specimens, quantitative DBTT data that are as accurate as those obtained using conventional ASTM E23 specimens. Work to date has focused on one-third or one-fourth size mini-CVN specimens

\*The work was performed during employment of Battelle.

[41–43]. In the present study, the specimen size is chosen close to the continuum limit of the material. For the ASTM A508 steel investigated, this results in a miniaturized specimen volume that is about one-sixteenth the volume of a conventional specimen.

## 2. Experimental procedure

The experimental design of the miniaturized fracture mechanics test was based on the material microstructure, current testing practice, amount of material available, and desired stress state. These design considerations are discussed in turn below.

### 2.1. Material microstructure

Material for this work was taken from a special heat of ASTM A508 steel provided by Oak Ridge National Laboratory for crack arrest research as part of the heavy section steel technology program. The steel has been extensively characterized at Oak Ridge as well as Battelle Columbus Division and the University of Maryland [44]. Conventional mechanical property and microstructural data are available for three different heat treatments, designated 6, 5A and 6R, in order of increasing toughness and increasing tempering temperature.

In order to confirm the data reported in [44], samples from the three heats were mounted and etched to enhance the ferritic grain structure. Micrographs were made, and the grain size was observed to be between 7.5 and 8.0 for ASTM designation G.

An important limitation in miniaturizing any specimen is the extent of the material's microstructural inhomogeneities. The usual guideline dictates that the specimen be at least five to ten times as large as the characteristic heterogeneity dimension. Microscopy analysis at the University of Maryland [44] (using heat treatment 5A) indicated that carbon segregates in slender bands about 0.25 mm wide. Examination by the Battelle Columbus Division metallography laboratory partly confirmed the existence of segregation, although the morphology was slightly different. Figure 1 is a low-magnification photomicrograph of the steel with heat treatment 6R. The dark regions are believed to be carbon-rich, reflecting an enhanced local density of carbide precipitates. Typical bands are shown at higher magnification in Fig. 2 for heat treatment 5A (intermediate temperature). Steel with the lowest tempering temperature (heat treatment 6) exhibited only faint indications of segregation. The reason for this difference is not clear. As a result of these findings, the minimum specimen dimension should be in the range of 3 to 5 mm. For a tensile specimen, this minimum size limits the diameter or thickness; for a fracture behaviour specimen, this minimum limits the dimensions of the crack plane.

### 2.2. Current testing practice

A number of ASTM standards relate to fracture mechanics testing of steel products [2–13]. Because of its relevance to the nuclear industry and compatibility with current in-service cutting techniques, the miniaturized notched bar specimen was chosen for examination. The specimen geometry was modified so that

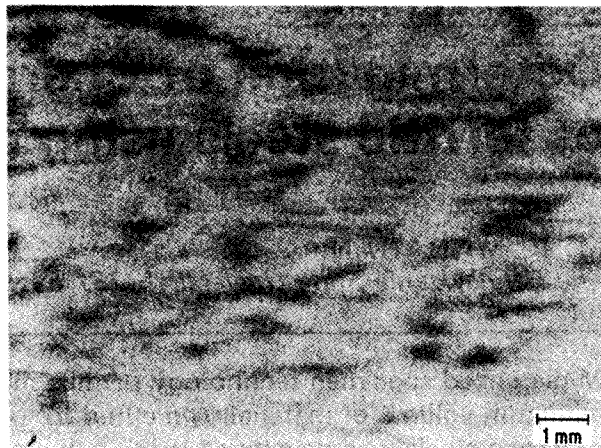


Figure 1 Low magnification micrograph of heat treatment 6R showing overview of carbon segregation.

fracture transition behaviour could be characterized using very small specimens.

The anvils were machined in accordance with [3]. All miniaturized specimen testing was performed statically. Conventional Charpy specimens were tested both statically and dynamically using a punch and anvil spacing as prescribed in [3]. For miniaturized specimens, it was necessary to decrease the punch thickness and anvil spacing. Key experimental parameters are compared in Table I. Other procedures and specifications regarding the test temperature, alignment accuracy, and machining tolerances were also in accordance with specifications in [3].

### 2.3. Material availability

The constraints on material volume in some future applications of the technology were considered in the design. The ratio of the volume of the ASTM standard compact-tension (CT) specimens to the volume of conventional TPB specimens is approximately 0.4. Therefore, the CT specimen is desirable based on a reduced volume criterion. However, the ratios of the thickness (crack plane), depth (direction of crack propagation), and length of the TPB specimen to those of the CT specimen are 1.0, 0.80 and 3.25, respectively. The TPB specimen may be more useful for semidestructive sampling, since it is difficult to

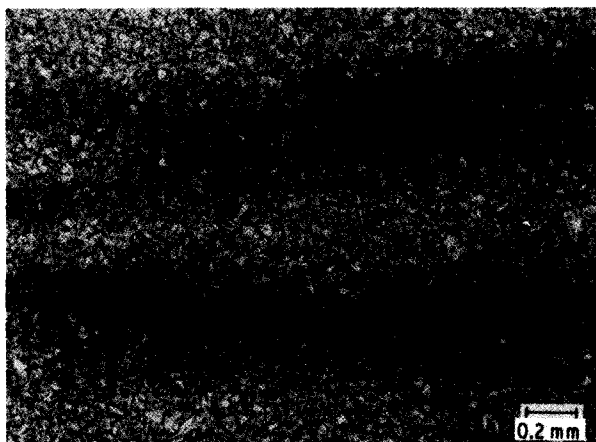
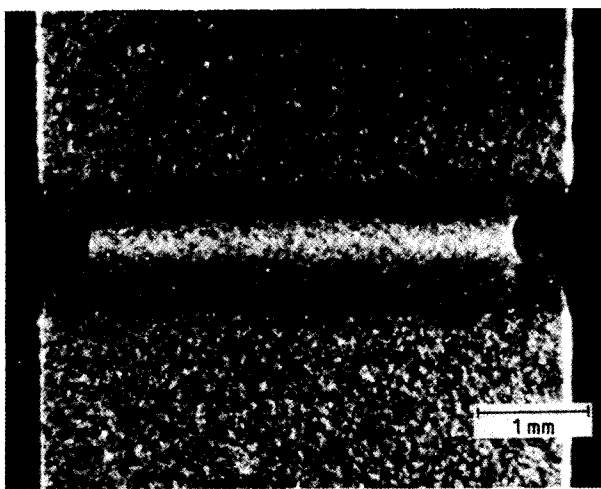


Figure 2 Higher magnification micrograph of segregation bands in heat treatment 5A.



veillance capsule and still satisfy the material-based size requirements for the steel being investigated.

## 2.4. Desired stress state

An important aspect of a fracture mechanics specimen design is the size effect. The stress field near the crack tip goes from an essentially triaxial (plane strain) to a biaxial (plane stress) field as the specimen thickness decreases. Since  $K_{Ic}$  is a function of only the material microstructure, it is the field parameter of interest. Plane stress and mixed mode fracture toughness ( $K_c$ ) depend on both geometrical and metallurgical factors.

The approach adopted in miniaturized specimen testing was to modify the specimen design to increase plastic constraint. In the current program, side grooves were machined into the specimen in addition to the notch, as shown in Fig. 3. The key miniaturized specimen design parameters are compared with conventional specimen parameters in Table II.

The effect of the side grooves is illustrated in Fig. 4. The  $\sigma_x$  stress component from the side groove in the thin sample is intended to offset the lack of the through-thickness stress  $\sigma_z$  that is present in the thick specimens. Although the  $\sigma_x$  stress in the miniaturized specimen is not, in general, uniformly distributed and is not of the same magnitude as the  $\sigma_z$  stress in the thick samples, sufficient constraint can be induced to enable measurement of the DBTT using miniaturized specimens. Historically, side grooving has been used to obtain more uniform crack fronts in fracture toughness testing and to constrain the fracture plane in certain materials. In the present study, the side grooves are brought into close proximity so that their  $\sigma_x$  stress components overlap; the result is a fairly uniform through-thickness stress field.

## 3. Data analysis and results

### 3.1. The load-displacement curve

At high test temperatures, the load-displacement curve (Path OABC, Fig. 5) passes through a maximum and then slowly declines (upper-shelf behaviour). The behaviour is a result of slow crack growth. At lower temperatures, a similar curve is observed, except that unstable cleavage fracture intervenes, resulting in curves OA1 and OAB2. The instability point shifts to lower displacements as the test temperature is lowered. This behaviour has been arbitrarily divided into two classes: (i) failure before the load peak in Fig. 5 (denoted by lower shelf); (ii) failure after the peak in Fig. 5 (denoted by upper shelf and transition).

TABLE II Comparison of key specimen dimensions

	ASTM Charpy specimen (mm)	Miniature specimen (mm)
Thickness, $B$ (crack plane)	10.01	4.83
Depth, $H$ (direction of crack propagation)	10.01	4.83
Length, $L$	54.99	12.70
Reduced side thickness, $B_n$	n/a	3.86
Notch depth, $a$	2.01	0.97
Notch-root radius, $r$	0.25	0.25

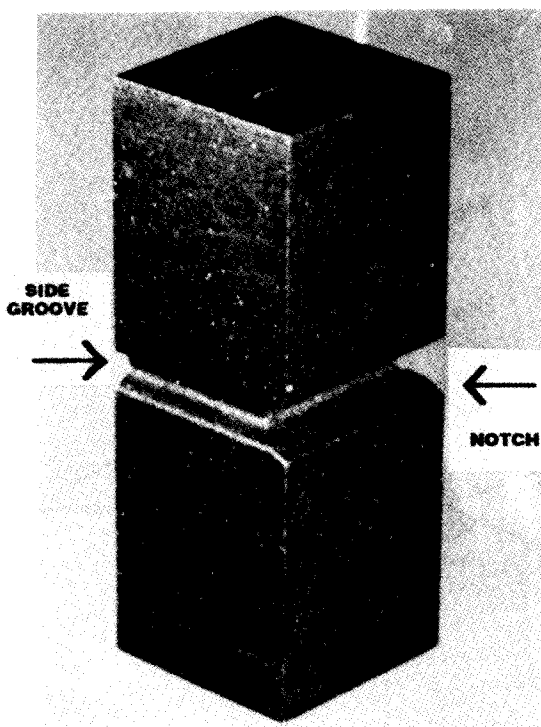


Figure 3 Miniaturized specimen showing side grooves and notch.

obtain a through-thickness crack-propagation specimen without cutting large, deeply penetrating pieces of material from the surface of a component for CT specimens. Therefore, miniaturized TPB specimens were chosen.

The miniaturized TPB specimens were sized so that eight specimens could be machined from each half of a conventional broken Charpy specimen. This permits the maximum number of specimens to be produced from a broken Charpy specimen from a nuclear sur-

TABLE I Comparison of key experimental parameters

	ASTM conventional Charpy (mm)	Miniature fracture mechanics (mm)
Punch radius	8.00	8.00
Punch tip width	3.99	2.29
Anvil radius	1.00	1.00
Anvil spacing	40.00	11.43

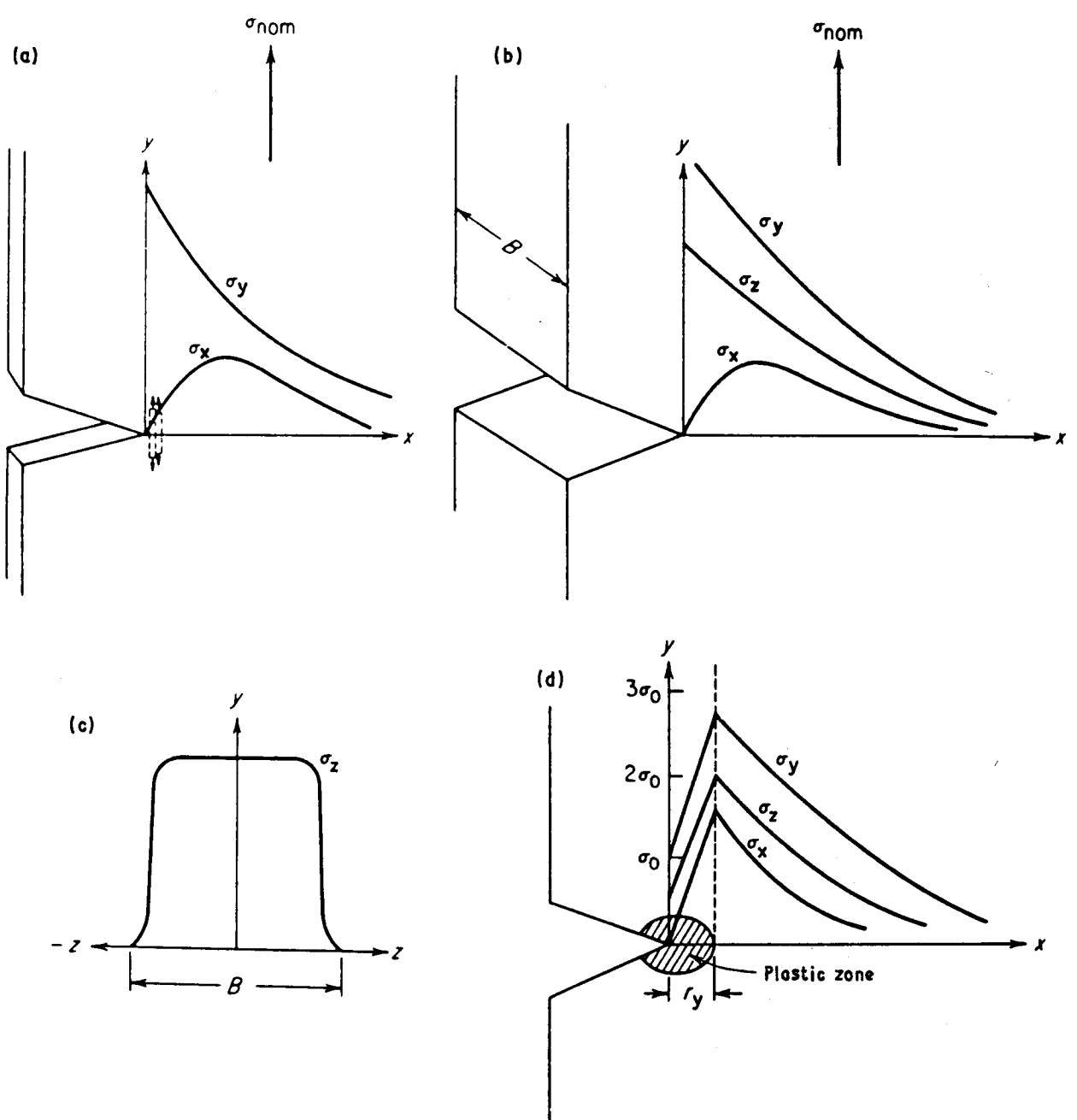


Figure 4 Schematic of crack tip stress fields [45].

### 3.2. Transition temperature shift

Several DBTT criteria are used in different industries. Since nuclear-grade steel was used in this study, the 41-J energy-absorption level was used as a reference. For the three heat treatments, the Charpy DBTTs are as follows: heat treatment 6, 40°C; heat treatment 5A, -7°C and heat treatment 6R, -29°C. Therefore, the key element of data interpretation is to be able to find a parameter and index that relates the miniature and conventional specimens. This parameter is defined as the range variable (for example, fracture appearance, lateral expansion) and the index as the transition temperature indicator (for example, 41-J, 0.89-mm lateral expansion). The results of this investigation are discussed below.

#### 3.2.1. Normalized energy

The first approach investigated was to normalize the energy parameter and the 41-J index. The absorbed energy was divided by the area of the crack plane in an

attempt to place the standard Charpy and miniaturized bend specimen data on a common basis. To allow a heat-to-heat comparison, all the test temperatures for the slow-bend specimens were adjusted by subtracting the appropriate impact-transition temperature. Fig. 6 shows the conventional Charpy specimen data normalized in this way. The normalizations provide good

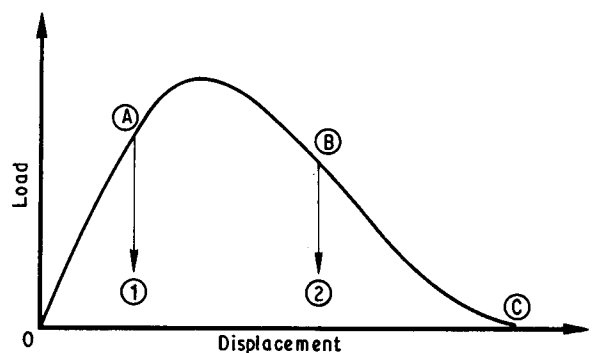


Figure 5 Schematic load-displacement curve.

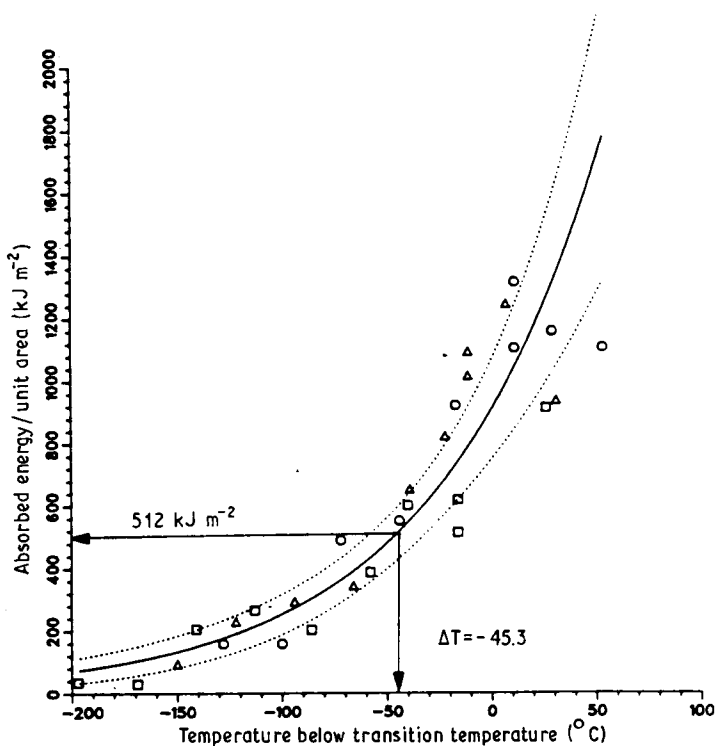


Figure 6 Energy absorbed in slow-bend fracture of standard Charpy specimens within the ductile–brittle transition region. □, Heat treatment 6; ○, heat treatment 6R; △, heat treatment 5A; —, Weibull fit; ···, 95% confidence limits.

superposition of the data, as expected. The 41-J ( $512 \text{ kJ m}^{-2}$ ) level occurs at about  $-45.3^\circ\text{C}$ . This factor accounts for the downward shift in the 41-J index due to testing statically. The data were fitted using the statistical analysis methodology reported in [46, 47]; ref. [48] presents a correlation for the temperature shift between slow-bend and impact loading. Using this correlation, the expected shift would be about  $36^\circ\text{C}$ . This is in reasonable agreement considering that the correlation in [48] is based on the assumption that the onset of the dynamic transition temperature is defined by the intersection of tangent lines drawn from the lower shelf level and the transition region.

Figure 7 shows the results for the miniaturized specimens. Two specimens at higher temperatures are off the scale of interest and consequently are not plotted. The superposition is again good at lower temperatures. The use of the miniaturized specimens results in a further downward shift of  $76.7^\circ\text{C}$  in temperature, producing a total shift of  $-122^\circ\text{C}$  between standard impact-Charpy tests and slow-bend miniaturized specimen tests. This result provides encouragement that miniaturized specimen procedures can yield DBTT data of comparable accuracy to those obtained using standard ASTM E23 procedures.

The miniaturized specimen data in Fig. 7 are scattered at higher temperatures due to experimental

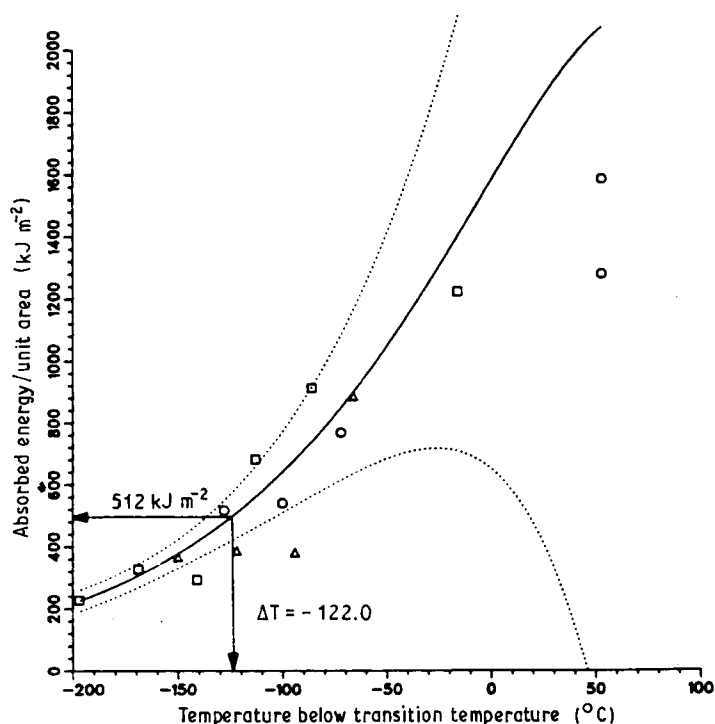


Figure 7 Energy absorbed in slow-bend fracture of miniaturized specimens within the ductile–brittle transition range. Symbols as Fig. 6.

difficulties. At higher temperatures, where there is stable crack growth and substantial plastic deformation, the specimens were observed to slip off the flat portion of the anvil and were supported by the curved portion. As a result, it was necessary to scale down the radius of curvature of the anvil and the punch. These changes are essential to measure high transition and upper-shelf data.

Tests were run without side-grooving the specimen, and the data in the transition region could not be analysed due to severe plastic deformation. Thus the experimental hurdle of DBTT testing near the material continuum limit has been overcome. However, to fully validate the test, the use of the normalized energy parameter and the  $512\text{-kJ m}^{-2}$  index was investigated to ensure consistency in fracture behaviour.

### 3.2.2. Fracture appearance

Further work was undertaken to solve the high transition region experimental difficulties mentioned earlier, and to investigate the fracture modes in the miniature specimens. In order for the miniature test to be valid, similar fracture behaviour to that obtained in the conventional 41-J specimen must be demonstrated. The punch and anvil dimensions were decreased to allow more bending at the higher temperature. A comparison of the conventional and miniature test specimen punch and anvil dimensions is given in Table III. The design modifications proved successful, and high-temperature miniature specimen data were obtained.

An interesting aspect of the fracture appearance is the shape of the crack front. The conventional Charpy specimens exhibit a convex crack front when viewed with the notch closest to the observer. This indicates that the stress intensity is highest near the centre of the specimen and the crack initiates near the centre of the notch. The miniature specimens show a concave crack front, suggesting that crack initiation occurs near the side grooves. The presence of the side grooves in the miniature specimens results in an increase in stress level near the side grooves, and the stresses are high enough to initiate the crack in this region of the specimen. Birbeck and Wraith [49] have shown that these crack-front shapes indicate that the appearance of the full-width crack at the notch root does not necessarily coincide with the maximum load. As discussed later, I have assumed this to be the case in all the calculations. In future work, crack initiation could be investigated experimentally using electric-potential (EP) techniques.

A planimeter was used to take fracture appearance measurements from photographs of the broken sur-

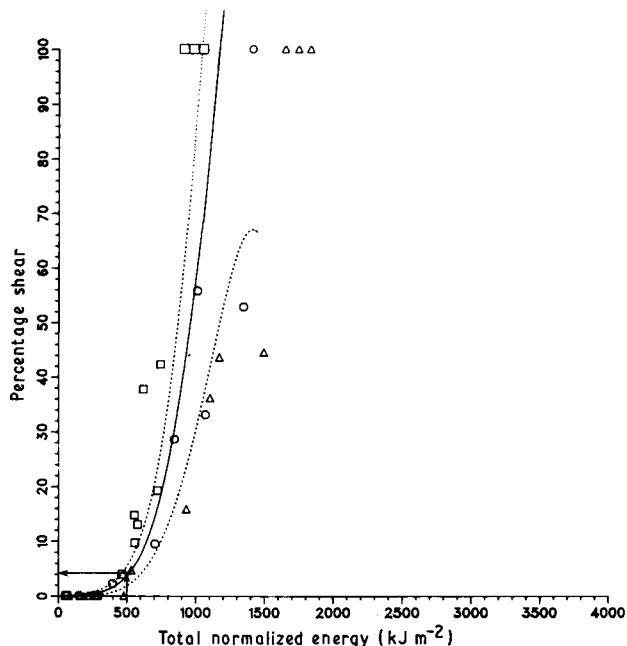


Figure 8 Normalized total energy as a fracture transition criterion (standard CVNs, all three materials).  $\square$ , Heat treatment 6;  $\circ$ , heat treatment 5A;  $\triangle$ , heat treatment, 6R; —, Weibull fit;  $\cdots$ , 95% confidence limits.

faces of the specimens. Due to the subjective nature of the usual methods of measurement, and the fact that it requires considerable effort to obtain accurate data, fracture appearance is not used in the nuclear industry as a measure of the ductile–brittle transition. Additionally, the regulations defining the transition temperature call for the energy-based 41-J index alone, and not for the measurement of the fracture appearance [50]. However, the measurement technique used in this study permits the use of fracture appearance as an accurate, quantitative measure of the brittle–ductile transition for both the miniature and conventional specimens.

The normalized energy data and the fracture appearance data were correlated using the MCFRAC code (Figs 8 and 9). As can be seen, it is possible to plot a single curve for the standard or the miniature specimens for all three materials. However, it is obvious that the curves for the two specimen types are not coincident for both the energy and normalized energy parameters. When the  $512\text{-kJ m}^{-2}$  index is used to compare the fracture appearance for both sizes of specimens based on the normalized energy parameter, it is apparent that  $512\text{ kJ m}^{-2}$  corresponds to approximately 4% shear fracture appearance for the standard specimens, but to about 1% shear for the miniature specimens.

If the total absorbed energy is compared in this way to fracture appearance, the disparity between the miniature and standard specimens is even greater (Figs 10 and 11). The miniature specimens at 41-J correspond to more than 70% shear, compared to about 4% for the standard specimens. It can be seen from a comparison of Figs 10 and 11 that the miniature specimens require less total energy to achieve a given value of percentage of shear than conventional CVNs. However, when the normalized energy is used, it is apparent that the miniature specimens seem to require more energy per unit fracture surface area to

TABLE III Relevant anvil support and punch dimensions

	Conventional Charpy test [ASTM81] (mm)	Miniature specimen test (phase 1 study) (mm)	Miniature specimen test (phase 2 study) (mm)
Punch radius	8.00	8.00	0.64
Punch tip width	3.99	2.29	1.27
Anvil radius	1.00	1.00	0.13
Anvil spacing	40.00	11.43	11.68

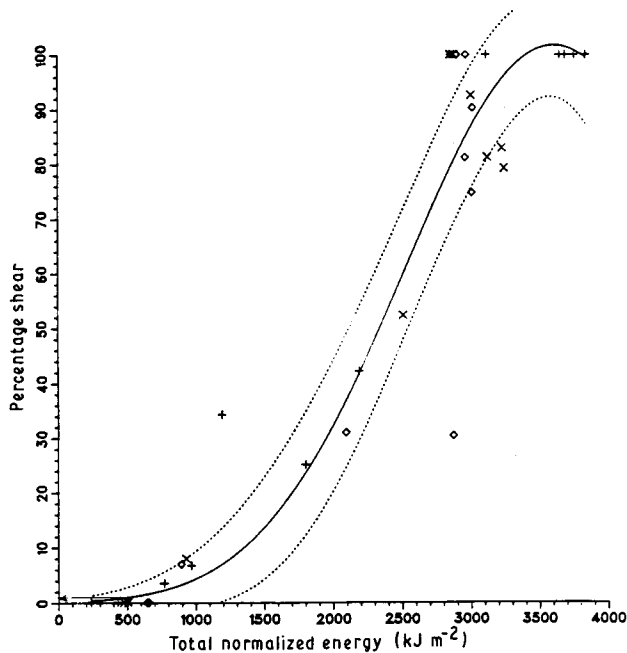


Figure 9 Normalized total energy as a fracture transition criterion (miniature CVNs, all three materials). +, Heat treatment 6; x, heat treatment 5A;  $\diamond$ , heat treatment 6R; —, Weibull fit;  $\cdots$ , 95% confidence limits.

achieve a given level of percentage of shear than do conventional CVNs. This observation suggests that the reasonable results obtained from using the energy normalization parameter are fortuitous, and may not hold for other materials. These results are summarized in Table IV.

These observations indicate that using normalized energy as a Charpy parameter and  $512 \text{ kJ m}^{-2}$  as a Charpy index for miniature specimens is not generally applicable. The reasonable data obtained thus far may be attributed to the fortuitously small difference in fracture appearance between standard and miniature specimens at the  $512\text{-kJ m}^{-2}$  level.

### 3.3. Fracture toughness

Published fracture toughness data [44] are available only for heat treatments 6 and 5A. This information was obtained principally at the Oak Ridge National Laboratory using two specimen types as follows:

1. Large cylinders ( $\sim 1.2\text{-m}$  length  $\times$   $1.0\text{-m}$  outer diameter  $\times$   $150\text{-mm}$  wall thickness) subjected to thermal shock.
2. Standard compact specimens ( $\sim 25\text{ mm}$  thick  $\times$   $60\text{ mm}$  square).  $K_{Ic}$  values for these specimens were reported using a thickness correction developed by Irwin *et al.* [51].

The fracture toughness data obtained from the current programme, which uses even smaller specimens, were

TABLE IV Percentage shear fracture appearance compared to energy (from Figs. 8–11)

	Percentage shear FA at $512 \text{ kJ m}^{-2}$	Percentage shear FA at 41 J
Standard specimens*	$\sim 4$	$\sim 4$
Miniature specimens*	$\sim 1$	$> 70$

\*All three materials.

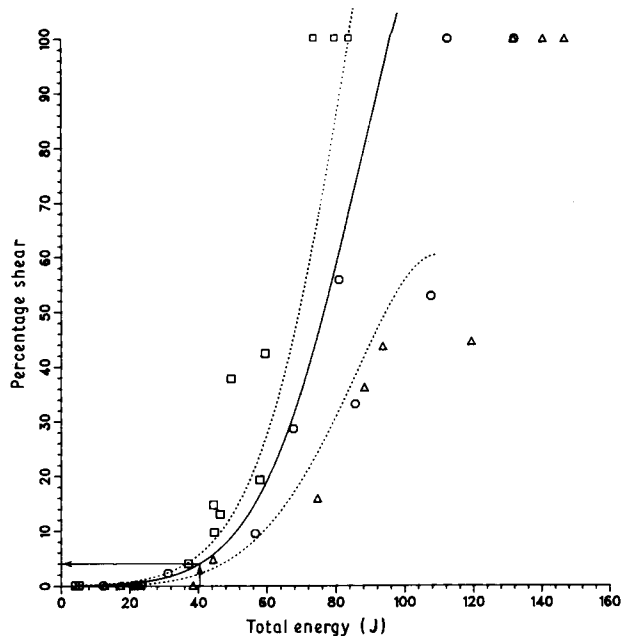


Figure 10 Non-normalized total energy as a fracture transition criterion (standard CVNs, all three materials). Symbols as Fig. 8.

corrected for side groove geometry and plasticity. In fracture mechanics testing, it is necessary to keep the plastic zone size small compared to the thickness, the uncracked ligament, and the crack length. Once the plastic zone becomes too large, the currently accepted fracture mechanics field parameters may not be appropriate. Also, the plastic zone size for plane strain is typically one-third of that for plane stress. Table V contains estimates of the plastic zone size for plane-strain conditions based on linear elastic fracture mechanics (LEFM). Table V also lists the ratio of the plastic zone size,  $r_y$ , to the specimen thickness,  $B$ , for the miniaturized specimens and Charpy specimens. The adjusted fracture toughness values reported in [52] were averaged at each temperature for heat treatment 6. ASTM E399 requires that  $r_y/B \leq 0.02$  to obtain valid  $K_{Ic}$  data [4]. As seen in Table V, this criterion is not met, and therefore a mixed mode condition likely exists over the temperature range tested.

In an attempt to obtain valid  $K_{Ic}$  data,  $K_{Ic}$  relations and correction factors not yet recommended by

TABLE V Plastic zone size estimates based on LEFM for heat treatment 6

Temperature ( $^{\circ}\text{C}$ )	Plastic zone size, $r_y$ (mm)	Ratio of $r_y$ to miniature specimen reduced thickness, $B_n$	Ratio of $r_y$ to Charpy specimen thickness, $B$
-73	0.31	0.08	0.03
-46	0.38	0.10	0.04
-32	0.58	0.15	0.06
-18	0.67	0.17	0.07
10	0.84	0.22	0.08
32	1.30	0.34	0.13
38	0.77	0.20	0.08
66	1.73	0.45	0.17
82	1.93	0.50	0.19
135	3.45	0.89	0.34

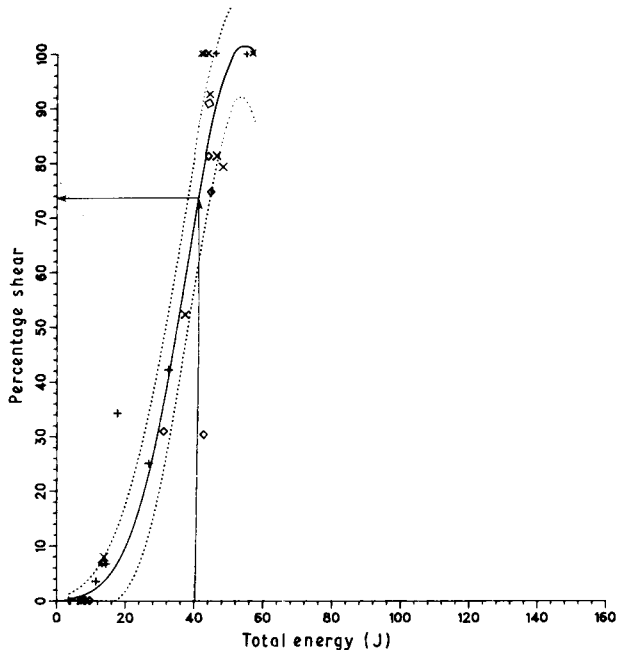


Figure 11 Non-normalized total energy as a fracture transition criterion (standard CVNs, all three materials). Symbols as Fig. 9.

ASTM were used. The general approach to testing methodology is to adhere to the guidance outlined in ASTM standards as much as possible [4, 5]. The basic elements of the data treatment are as follows:

1. Use Srawley's [53] wide-range stress-intensity factor expression to calculate the driving force for fracture.
2. Apply a geometry correction to account for the side grooves.
3. Assume that the elastic stored energy is the only energy available to drive a cleavage crack.
4. Adjust the apparent fracture toughness values obtained by applying a size correction.

Elements 1 and 2 above are well known and established within the fracture mechanics community. Elements 3 and 4 are among those being considered by ASTM standard subcommittees and must be characterized as controversial. For the side-grooved miniaturized specimens, the correction factor  $B/B_n$  was

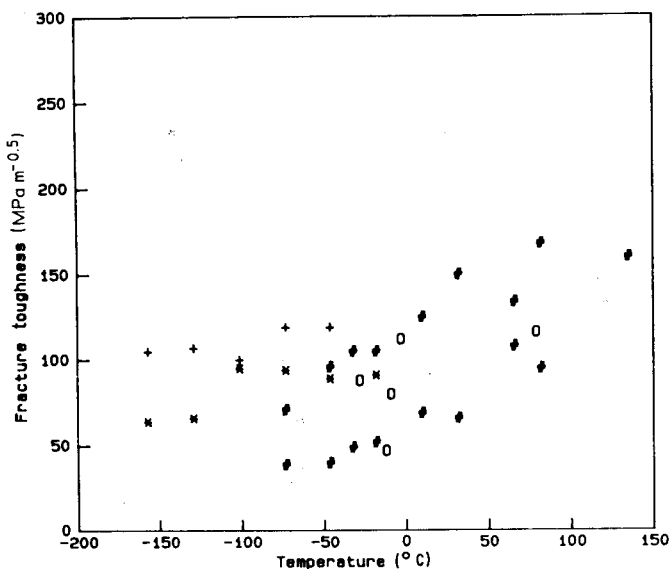


Figure 12 Fracture toughness; heat treatment 6.  $\circ$ , Cylinders, thermal shock;  $\#$ , compact specimens (1T);  $*$ , Charpy specimens;  $+$ , miniature bend specimens.

applied to account for the geometry change. In the present study, element 4 was not used.

Rosenfield and Shetty's [54] energy correction method was used. The argument is that the energy expended in stable growth is not available to drive the unstable crack. Therefore, the influence of this energy must be eliminated from the experimental record if the data are to be representative of a large vessel where stable growth is unlikely to occur because of the geometrical constraint.

Only the lower transition specimens are included in the comparison because of uncertainties in analysing the other data. Figs 12 and 13 show small specimen toughness data compared to the Oak Ridge larger-specimen data. Both figures indicate the extent to which the Charpy and miniaturized-specimen procedures succeeded. Figure 12 shows that cleavage failure was achieved in the Charpy specimen at a temperature which overlaps both the 1T and cylinder data for heat treatment 6. The miniaturized data overlapped only the 1T results. Even so, both designs produced data that were on the high (non-conservative) edge of the simulated vessel scatter band. In Fig. 13, for heat treatment 5A, temperature overlap was not achieved and the data also appear to be high. Possibilities for approaching plane-strain conditions further using miniaturized specimens include:

1. Fatigue precracking the specimens in accordance with standard procedures.
2. Side-grooving the Charpy specimen as the miniaturized specimen has been. This alternative has the advantage of economy at the sacrifice of size. Some savings in material (a factor of three) could be achieved if a reconstitution procedure is used whereby arms are welded onto the centre sections of Charpy specimens.
3. Loading at higher rates, to obtain some decrease in toughness to approach lower bound values.

#### 4. Conclusions and recommendations

The miniaturized specimen design required only 6% of the volume of a standard Charpy specimen. These specimens have proved satisfactory for estimating

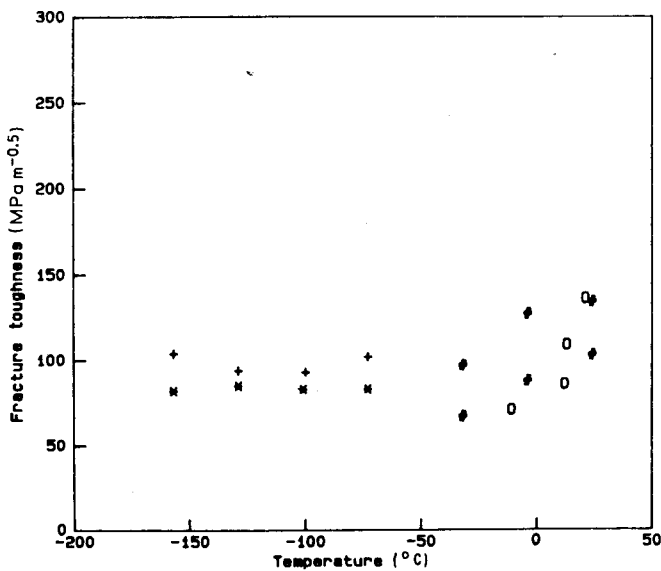


Figure 13 Fracture toughness; heat treatment 5A. Symbols as in Fig. 12.

transition temperature shifts due to heat treatment of a reactor-grade pressure vessel steel. Fracture appearance has been demonstrated to be a useful miniature specimen parameter. For applications in the nuclear industry, conventional dynamic A508 steel Charpy specimens exhibit approximately 4% shear at the 41-J energy level. Therefore, the appropriate index for miniature specimens is 4% shear for this material. The  $512\text{-kJ m}^{-2}$  index was found to be useful with the A508 steel studied; however, future use of this index requires a fracture mode investigation. It is recommended that the research be extended to include several irradiated structural steels and weldments. Additional work is needed to obtain high transition behaviour data. Of key importance to complete validation of the method has been a careful investigation of fracture modes in the miniaturized specimens.

High fracture toughness values were obtained using the miniaturized specimens, even after appropriate adjustments were applied. Specimen and test procedure modifications may lead to characteristically low toughness values.

### Acknowledgements

I would like to express my thanks to Battelle's Office of Corporate Technical Development for sponsorship of this work. I am also grateful to J. A. VanECHO and C. Charles for assistance in the experimental portion of the programme, and to A. R. Rosenfield who performed a share of the work and made several helpful suggestions.

### References

1. M. P. MANAHAN, A. S. ARGON and O. K. HARLING, US Patent 4567774, February (1986). (A further improvement patent is pending.)
2. ASTM Standard A370-86a, Mechanical testing of steel products (American Society for Testing and Materials, Philadelphia, 1986).
3. ASTM Standard E23-86, Notched bar impact testing of metallic materials (American Society for Testing and Materials, Philadelphia, 1986).
4. ASTM Standard E399-83, Plane-strain fracture toughness of metallic materials (American Society for Testing and Materials, Philadelphia, 1983).
5. ASTM Standard E813-81, Test method for  $J_{Ic}$ , a measure of

- fracture toughness (American Society for Testing and Materials, Philadelphia, 1985).
6. ASTM Standard E436-74, Drop-weight tear tests of ferritic steels (American Society for Testing and Materials, Philadelphia, 1974).
7. ASTM Standard 338-78, Sharp-notch tension testing of high-strength sheet materials (American Society for Testing and Materials, Philadelphia, 1974).
8. ASTM Standard E602-81, Sharp-notch tension testing with cylindrical specimens (American Society for Testing and Materials, Philadelphia, 1981).
9. ASTM Standard E604-83, Dynamic tear testing of metallic materials (American Society for Testing and Materials, Philadelphia, 1983).
10. ASTM Standard E740-80, Fracture testing with surface-crack tension specimens (American Society for Testing and Materials, Philadelphia, 1980).
11. ASTM Standard E561-86, R-Curve determination (American Society for Testing and Materials, Philadelphia, 1986).
12. ASTM Standard E616-80, Fracture testing (American Society for Testing and Materials, Philadelphia, 1980).
13. ASTM Standard E208-85, Conducting drop-weight test to determine nil-ductility transition temperature of ferritic steels (American Society for Testing and Materials, Philadelphia, 1985).
14. C. W. MacGREGOR, N. GROSSMAN and P. R. SHEPLER, *Weld. J. Res. Suppl.* January (1947) 50-s.
15. *Idem, ibid.* January (1948) 7-s.
16. R. S. ZENO and J. R. LOW, *ibid.* March (1948) 145-s.
17. E. SMITH and B. M. PATCHETT, *ibid.* June (1975) 169-s; July (1975) 226-s.
18. D. FIRRAO *et al.*, *Metall. Trans.* **13A** (1982) 1003.
19. W. F. BROWN, Jr, J. D. LUBAHN and L. J. EBERT, *Weld. J. Res. Suppl.* October (1947) 554-s.
20. N. DAVIDENKOV, C. SHEVANDIN and F. WITTMAN, *Trans. ASME* **69** (1947) 63.
21. F. JONASSEN, *Weld. J. Res. Suppl.* January (1948) 27-s.
22. W. M. WILSON, R. A. HECHTMAN and W. H. BRUCKNER, *ibid.* April (1948) 200-s.
23. D. C. BUFFUM, *ASTM Bull.* **TP 143** (1949) 45.
24. C. W. MacGREGOR and N. GROSSMAN, *Weld. J. Res. Suppl.* January (1952) 20-s.
25. G. R. IRWIN, in "Symposium on Effect of Temperature on Brittle Behaviour of Metals with Particular Reference to Low Temperatures", ASTM-STP 158 (ASTM, Philadelphia, 1953).
26. H. SCHWARTZBART and J. P. SHEEHAN, *ASTM Proc.* **54** (1954) 939.
27. G. N. ORNER and C. E. HARTBOWER, *Weld. J. Res. Suppl.* December (1957) 521-s.
28. M. GROUND, in "Effects of Radiation on Structural Metals", ASTM-STP 426 (ASTM, Philadelphia, 1967) p. 224.

29. O. L. TOWERS, *Metal Const.* **15** (1983) 682.
30. S. T. ROLFE and J. M. BARSOM, in "Fracture and Fatigue Control in Structures: Applications of Fracture Mechanics" (Prentice-Hall, New Jersey, 1971).
31. S. L. HOYT, *ASTM Proc.* **38** (1938) 162.
32. E. P. KLIER, F. C. WAGNER and M. GENSAMER, *Weld. J. Res. Suppl.* February (1948) 71-s.
33. R. RARING, *ASTM Proc.* **52** (1952) 1034.
34. J. E. DEGRAAF and J. H. VAN DER VEEN, *J. Iron Steel Inst.* January (1953) 19.
35. C. W. MacGREGOR and N. GROSSMAN, *Weld. J. Res. Suppl.* January (1948) 16-s.
36. C. W. MacGREGOR and N. GROSSMAN, *ibid.* March (1948) 159-s.
37. C. E. HARTBOWER and W. S. PELLINI, *ibid.* July (1950) 348-s.
38. W. J. HARRIS Jr., J. A. RINEBOLT and R. RARING, *ibid.* September (1951) 417-s.
39. C. E. HARTBOWER, *ASTM Proc.* **54** (1954) 929.
40. *Idem*, *Weld. J. Res. Suppl.* May (1957) 85-s.
41. W. R. CORWIN and A. M. HOUGHLAND, in "The Use of Small-Scale Specimens for Testing Irradiated Material", ASTM-STP 888, edited by W. R. Corwin and G. E. Lucas (ASTM, Philadelphia, 1986) p. 337.
42. G. E. LUCAS, G. R. ODETTE, J. W. SHECKHERD, P. McCONNELL and J. PERRIN, in *ibid.*, p. 322.
43. P. McCONNELL, J. W. SHECKHERD, J. S. PERRIN and R. A. WULLAERT, in *ibid.*, p. 367.
44. R. D. CHEVERTON *et al.*, in "Pressure Vessel Fracture Studies Pertaining to the PWR Thermal-Shock Issue: Experiments TSE-5, TSE-5A and TSE-6". Oak Ridge National Laboratory NUREG/CR-4249 ORNL-6163 report to US Nuclear Regulatory Commission.
45. G. E. DIETER, in "Mechanical Metallurgy", 2nd edn (McGraw-Hill, New York, 1976) p. 281.
46. M. P. MANAHAN, A. R. ROSENFELD and S. F. QUAYLE, in "Statistical Methodology for Analysis of Fracture Mechanics Data". Final Report from Battelle-Columbus to Corporate Technical Development, January 31, 1985.
47. M. P. MANAHAN, S. QUAYLE, A. R. ROSENFELD and D. K. SHETTY, in "Statistical Analysis of Cleavage-Fracture Data", presented at the International Conference and Exhibition on Fatigue, Corrosion Cracking, Fracture Mechanics and Failure Analysis, Salt Lake City, December 2-6, 1985, edited by V. S. Goel (American Society for Metals) pp. 495-500.
48. S. T. ROLFE and J. M. BARSOM, in "Fracture and Fatigue Control in Structures" (Prentice Hall, New Jersey, 1977).
49. G. BIRBECK and A. E. WRAITH, in "Influences of Crack Shape or Crack Opening Displacement Measurements Using Charpy Specimens" ASTM STP 466 (ASTM, Philadelphia, 1970) p. 281.
50. United States Office of the Federal Register, Code of Federal Regulations, 10 "Energy" (Washington, DC, 1979).
51. G. R. IRWIN, J. M. KRAFT and A. A. WELLS, in "Basic Aspects of Crack Growth and Fracture" (Naval Research Laboratory, NRL Report 6598, 1967).
52. J. G. MERKLE, in "An Examination of the Size Effects and Data Scatter Observed in Small-Specimen Cleavage Fracture Toughness Testing", Oak Ridge National Laboratory, NUREG/CR-3672 ORNL/TM-9088 (1984).
53. J. E. SRAWLEY, *Int. J. Fracture* **12** (1976) 475.
54. A. R. ROSENFELD and D. K. SHETTY, in "Elastic-Plastic Fracture Test Methods: The User's Experience", ASTM STP 856, edited by E. T. Wessel and F. J. Loss (ASTM, Philadelphia, 1984) p. 196.

*Received 28 September 1988  
and accepted 28 February 1989*